

# We are IntechOpen, the world's leading publisher of Open Access books Built by scientists, for scientists

6,900

Open access books available

186,000

International authors and editors

200M

Downloads

Our authors are among the

154

Countries delivered to

TOP 1%

most cited scientists

12.2%

Contributors from top 500 universities



WEB OF SCIENCE™

Selection of our books indexed in the Book Citation Index  
in Web of Science™ Core Collection (BKCI)

Interested in publishing with us?  
Contact [book.department@intechopen.com](mailto:book.department@intechopen.com)

Numbers displayed above are based on latest data collected.  
For more information visit [www.intechopen.com](http://www.intechopen.com)



# Development of a Vectored Water-Jet-Based Spherical Underwater Vehicle

Shuxiang Guo and Xichuan Lin  
*Kagawa University*  
*Japan*

## 1. Introduction

The applications of underwater vehicles have shown a dramatic increase in recent years, such as, mines clearing operation, feature tracking, cable or pipeline tracking and deep ocean exploration. According to different applications, the mechanical and electrical configuration and shape of an underwater vehicle are different. For instance, manipulators are necessary when doing mines clearing operation or some other tasks which need to deal with environment. If an underwater vehicle is used for underwater environment detection or observation, it is better to make this vehicle smaller and flexible in motion that it can go to smaller space easily. If the vehicle needs high speed moving in the water then a streamline body is required.

Different structures with different size of underwater vehicles are developed. Most of these underwater vehicles are torpedo-like with streamline bodies, like (Sangekar et al., 2009). And there are some small size AUVs like (Allen et al., 2002) and (Madhan et al., 2006). And also there are some other AUVs adopt different body shape, such as (Antonelli & Chiaverini, 2002). Meanwhile, the propulsion system is one of the critical facts for the performance of underwater vehicles, because it is the basis of control layers of the whole system. Propulsion devices have variable forms, for instance, paddle wheel, poles, magneto hydrodynamic drive, sails and oars.

Paddle wheel thrusters are the most common and traditional propulsion methods for underwater vehicles. Usually, there are at least two thrusters installed on one underwater vehicle, one for horizontal motion and the other for vertical motion. The disadvantages of paddle wheel thrusters are obvious, for example, it is easy to disturb the water around the underwater vehicles. Meanwhile, the more the paddle wheel thrusters are used, the weight, noise and energy consumption increases.

The steering strategies of traditional underwater vehicles are changing the angular of rudders or using differential propulsive forces of two or more than two thrusters. Of course, there are vectored propellers being used on underwater vehicles. Reference (Cavallo et al., 2004) and (Le Page & Holappa, 2002a) present underwater vehicles with vectored thrusters. Reference (Duchemin et al., 2007) proposes multi-channel hall-effect thrusters which involves vector propel and vector composition. Reference (Le Page & Holappa, 2002b) proposes an autonomous underwater vehicle equipped with a vectored thruster. At the same time, the design of vectoring thrusters used on aircrafts is also an example of vectored propulsion system (Kowal, 2002), (Beal, 2004) and (Lazic & Ristanovic, 2007).

The purpose of this research is to develop such a kind of underwater vehicle which can adjust its attitude freely by changing the direction of propulsive forces. Meanwhile, we would like to make the vehicle flexible when moving in the water. Inspired by jet aircraft, we adopt vectored water-jet propellers as the propulsion system. According to the design purpose, a symmetrical structure would be better for our underwater vehicle (Guo et al., 2009).

This spherical underwater vehicle has many implementation fields. Because of its flexibility, our vehicle can be used for underwater creatures observation. For example, we can install underwater cameras on the vehicle. It can track and take photos of fishes. Another example is that, due to its small size, we can use it to detect the inside situation of underwater oil pipes.

## 2. Mechanical and electrical design

### 2.1 Mechanical system design

Before the practical manufacture, we try to give a conceptual design of the whole structure for this spherical underwater vehicle. At this stage, we need to consider about the dimension, weight distribution, material, components installation, and so on. And we also need to consider about the configuration of the propulsion system, for example, how many water-jet propellers should we use for the purpose of optimizing power consumption without decreasing propulsion ability. Therefore, by all of that mentioned above, we give the conceptual designed structure of our spherical underwater vehicle as shown in Fig.1.

It adopts a spherical shape, all the components are installed inside the body. Its radius is 20cm which is smaller than that in (Antonelli et al., 2002). Its overall weight is about 6.5kg. Its working depth is designed to 0-10m, with a max speed of about 1.5m/s.

Inside the vehicle, there will be three water-jet propellers used as propulsion system, which is enough for surge, yaw and heave. One waterproof box is used for all the electronic components such as sensors, batteries and the control boards. And all of these are mounted on a triangle support which is fixed on the spherical hull. The whole structure is symmetrical in z-axis. Therefore, it can rotate along z-axis, and by doing this, the vehicle can change its orientation easily.

#### 2.1.1 The spherical hull

As shown in Fig.2, the spherical hull of this underwater vehicle is made of acrylic which is light and easy to be cut. It is about 3mm thick and the diameter is 40cm. Actually, we can see that this spherical hull is composed of two transparent hemisphere shells. There are three holes which can provide enough space for water-jet propellers to rotate for different motions. We will discuss the details about the principles of the water-jet propulsion system in the next section.

#### 2.1.2 The waterproof box

Waterproof is essential for underwater vehicles. Fig.3 shows the design of the waterproof box. The whole size of this box is about 22cm(height) × 14cm(inner diameter). An O-ring is used for seal, which has the ability to provide waterproof in our case. Inside the waterproof box, there will be two control boards, one or two lithium batteries, depending on tasks. Meanwhile, at the top part inside the box, there will be a digital rate gyro sensor for orientation feedback. The body of waterproof box is also transparent, therefore, we can easily observe the inside working status.

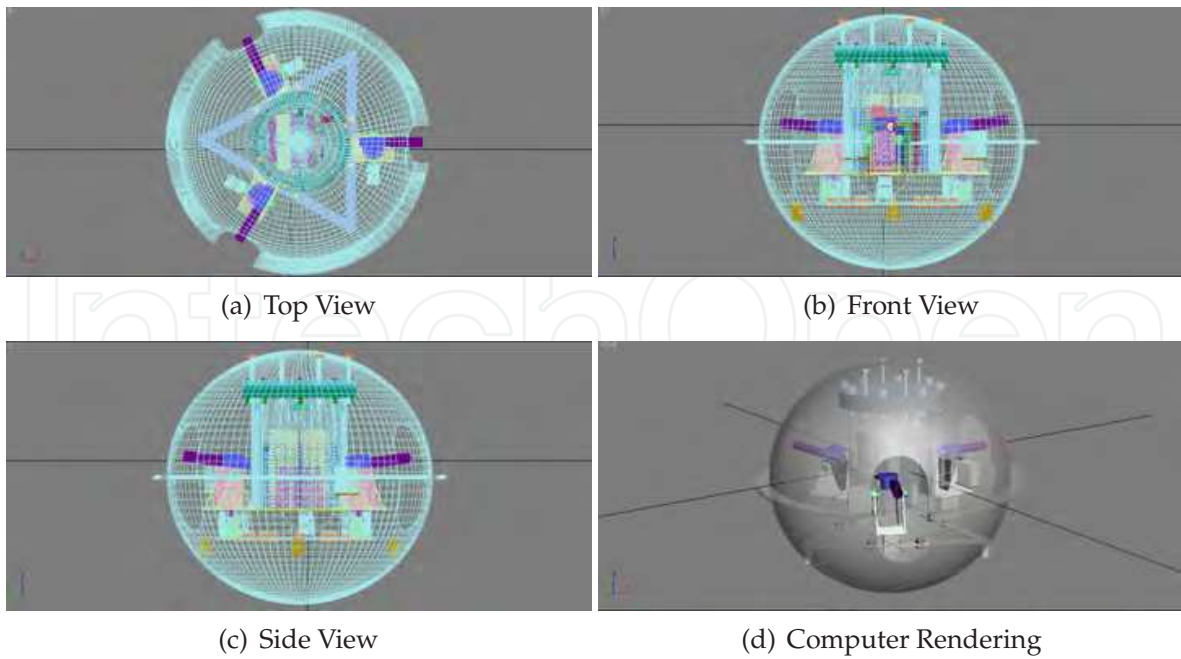


Fig. 1. Mechanical System Schematics of the Spherical Underwater Vehicle

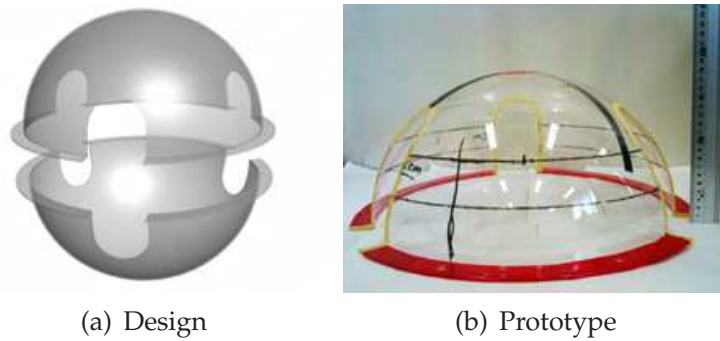


Fig. 2. Spherical Hull

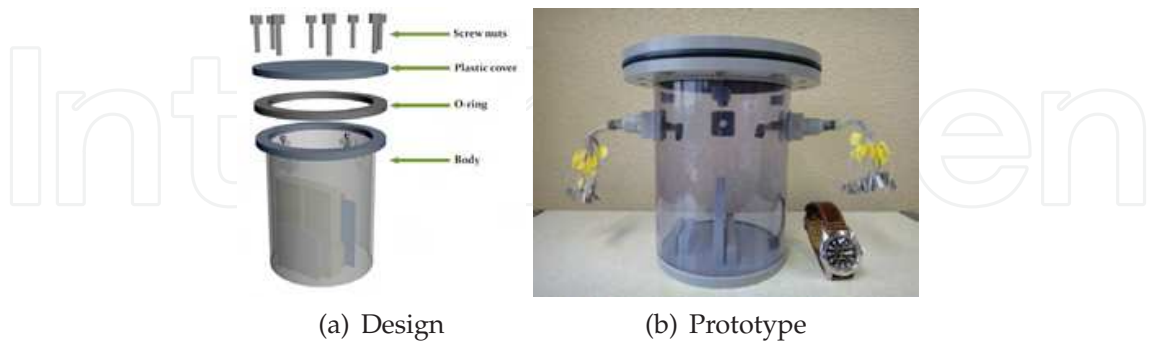


Fig. 3. Design of Waterproof Box

**2.1.3 Mechanism of the water-jet propulsion system**

Fig.4 is the structure of one single water-jet propeller. It is composed of one water-jet thruster and two servo motors (above and side). The water-jet thruster is sealed inside a plastic box for waterproof. And we use waterproof glue on servo motors for waterproof. The thruster can be

rotated by these two servo motors, therefore, the direction of jetted water can be changed in X-Y plane and X-Z plane, respectively.

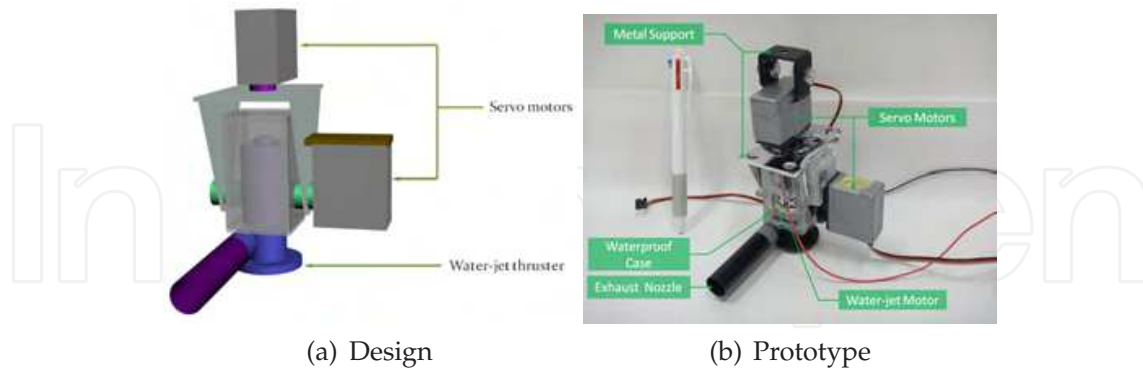


Fig. 4. Structure of a Water-jet Propeller

Three of the water-jet propellers are mounted on the metal support frame, as shown in Fig.5. Three of them are circumferentially  $2\pi/3$  apart from each other.

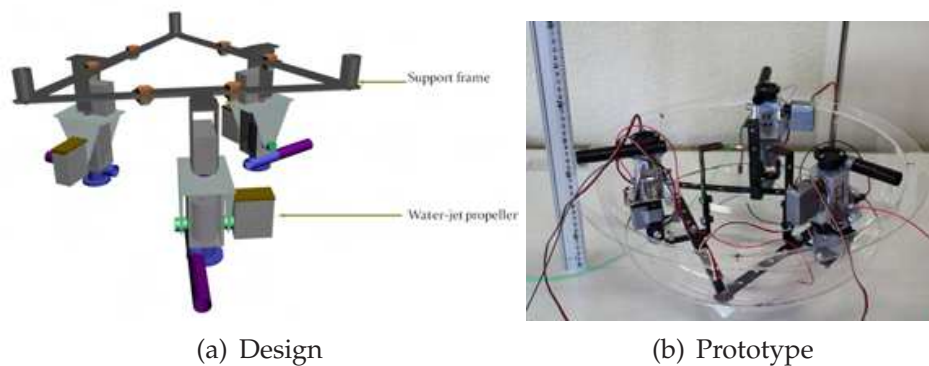


Fig. 5. Water-jet Propellers mounted on Support Frame

## 2.2 Electrical system design

We adopt a minimal hardware configuration for the experimental prototype vehicle. For a single spherical underwater vehicle, there are three major electrical groups, sensor group, control group and actuator group. Fig.6 gives the electrical schematics. At present, we only use one pressure sensor for depth control and one gyro sensor for surge control. One ARM7 based control board is used as central control, data acquisition, algorithm implement and making strategic decisions. One AVR based board is used as the coprocessor unit for motor control. It receives the commands from ARM and translates the commands into driving signals for the water-jet propellers.

Fig.7 gives the main hardware for this vehicle. Fig.7(a) is the ARM7 based board with S3C44B0X on it, which can fulfill our requirement at present. Fig.7(b) is the AVR based board with ATmega2560 on it. RS232 bus is used for the communication between ARM7 and AVR. In Fig.7(c) is the set of pressure sensor with the sensor body(right) and its coder (left). It use RS422 bus for data transmission. Digital gyro sensor CRS10 is shown in Fig.7(d), we use the build in AD converter of S3C44B0X for data acquisition.

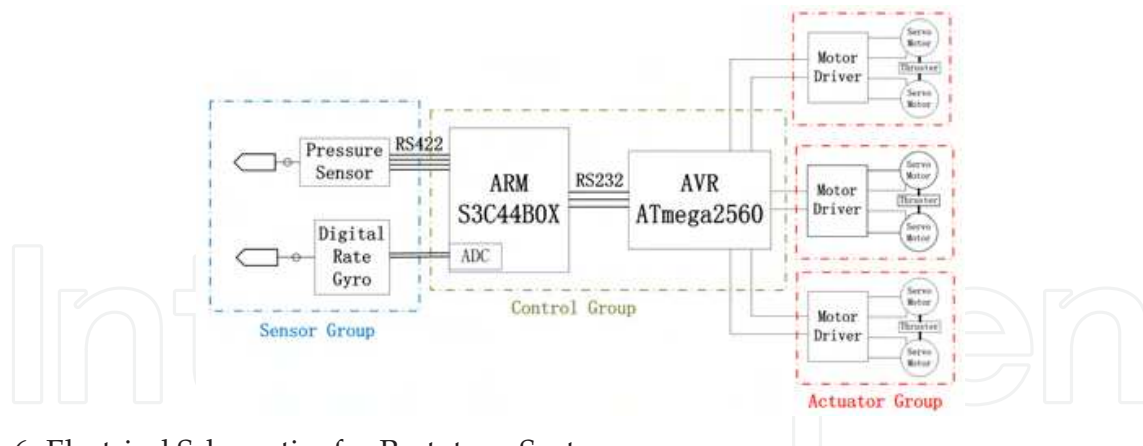
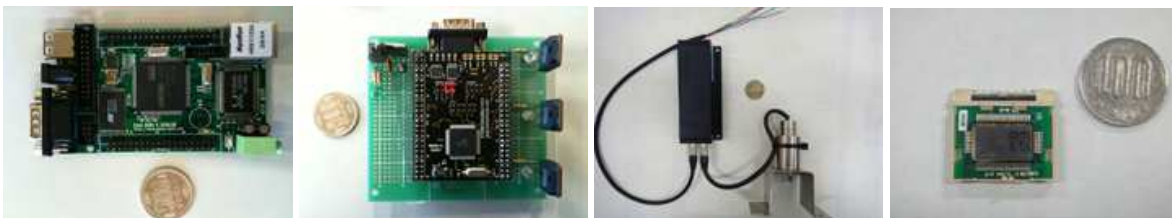


Fig. 6. Electrical Schematics for Prototype System



(a) S3C44B0X Board (b) ATmega2560 Board (c) Pressure Sensor (d) Gyro Sensor

Fig. 7. Electrical Components for the Experimental Prototype Underwater Vehicle

### 2.3 Power supply

We adopt two power supply for the spherical underwater vehicle. The highest power consumption components in our vehicle are propellers. For each of them, the thruster has a working voltage of 7.2V and 3.5A current drain, servo motors can work under 5V with relatively small current. Therefore, we use two 2-cells LiPo batteries as the power supply for the propellers. The capacity of each battery is 5000mAh with parameter of 50c – 7.4V. Besides, we use 4 AA rechargeable batteries for the control boards. We carried out the power consumption test for one LiPo battery, and Fig.8 gives the battery discharge graph of the power system.

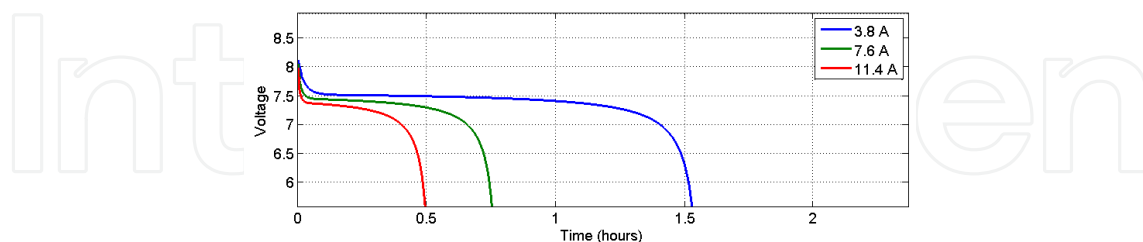


Fig. 8. Power Consumption of the Whole System. Blue line – one propeller working; green line – two propellers working; red line – three propellers working

### 3. Principles and modeling of the propulsion system

In this section, we will discuss about the working principles, modeling method and the identification experiment for the water-jet propeller. Many literatures have presented the computing formula for the torque and thrust exerted by a thruster. Most of them are base on

the lift theory, and mainly focus on blades type propellers (Newman, 1977), (Fossen, 1995) and (Blanke et al., 2000). Our propellers are different with blades type propellers, therefore, we try to find another method for the modeling of water-jet propellers. In (Kim & Chung, 2006), the author presented a dynamic modeling method in which the flow velocity and incoming angle are taken into account. We will use this modeling method for our water-jet propellers.

### 3.1 Working principles

Before modeling of propulsion system, we want to give some basic working principles about the water-jet propellers. Fig.9(a) shows the top view of distribution of three propellers. They can work together to realize different motion, such as surge and yaw.

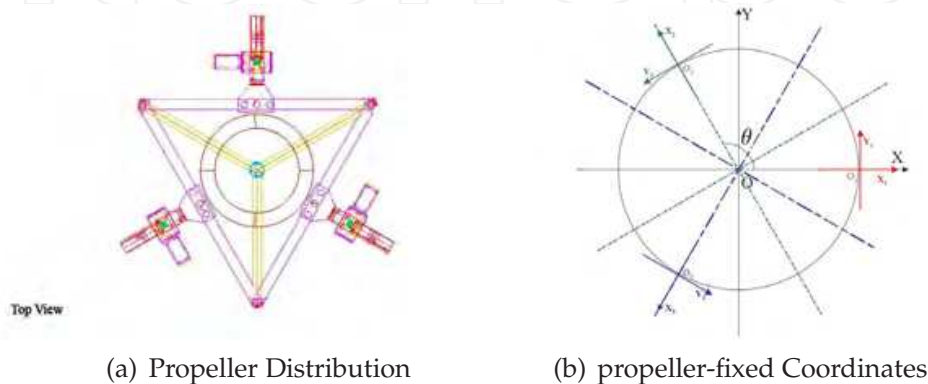


Fig. 9. Distribution and Coordination of Multiple Propellers

If we let  $\theta$  be the interval angle of each water-jet propeller, as shown in Fig.9(b), then, for the purpose of kinematics transform, three propeller-fixed coordinates are introduced for propellers, which are fixed in the rotation center of the propellers. So we can see, these three propeller-fixed coordinates are actually transform results of vehicle-fixed coordinate reference frame. Meanwhile, it should be noted that, this transform only happens in  $X$ - $Y$  plane. Let the matrix form of the coordinates transform be given as:

$$\begin{pmatrix} X_1 \\ Y_1 \\ Z_1 \end{pmatrix} = \begin{pmatrix} X \\ Y \\ Z \end{pmatrix} + \begin{pmatrix} -R \\ 0 \\ 0 \end{pmatrix} \quad (1)$$

$$\begin{pmatrix} X_2 \\ Y_2 \\ Z_2 \end{pmatrix} = \begin{pmatrix} c\theta & s\theta & 0 \\ -s\theta & c\theta & 0 \\ 0 & 0 & 1 \end{pmatrix} \begin{pmatrix} X \\ Y \\ Z \end{pmatrix} + \begin{pmatrix} \frac{1}{2}Rc\theta - Rs\theta c\frac{\pi}{6} \\ -\frac{1}{2}Rc\theta - Rc\theta c\frac{\pi}{6} \\ 0 \end{pmatrix} \quad (2)$$

$$\begin{pmatrix} X_3 \\ Y_3 \\ Z_3 \end{pmatrix} = \begin{pmatrix} c2\theta & s2\theta & 0 \\ -s2\theta & c2\theta & 0 \\ 0 & 0 & 1 \end{pmatrix} \begin{pmatrix} X \\ Y \\ Z \end{pmatrix} + \begin{pmatrix} \frac{1}{2}Rc2\theta + Rs2\theta c\frac{\pi}{6} \\ -\frac{1}{2}Rc2\theta + Rc2\theta c\frac{\pi}{6} \\ 0 \end{pmatrix} \quad (3)$$

where  $R$  is the radius of the vehicle,  $s(\cdot) \equiv \sin(\cdot)$  and  $c(\cdot) \equiv \cos(\cdot)$ .

So, a general transform matrix can be obtained:

$${}^p P_b = \Phi_p^b \cdot {}^p P_p + C \quad (4)$$

where  ${}^p P_b$  is the position vector of propeller-fixed coordinate expressed in vehicle-fixed coordinate,  $\Phi_p^b = (\Phi_{p1}^b, \Phi_{p2}^b, \Phi_{p3}^b)^T$  is the transform matrix from propeller-fixed coordinate to vehicle-fixed coordinate,  ${}^p P_p$  is the position vector in propeller-fixed coordinate and the  $C$  is a constant vector.

Now, let us take a look at three motions, surge, heave and yaw. The definition of these three motions can be found in (Fossen, 1995). Before that, we define two angles which will be used for orientation of propellers. Fig.10 gives the definition of  $\alpha$  and  $\beta$ . Fig.11 gives a demonstration of surge, heave and yaw.

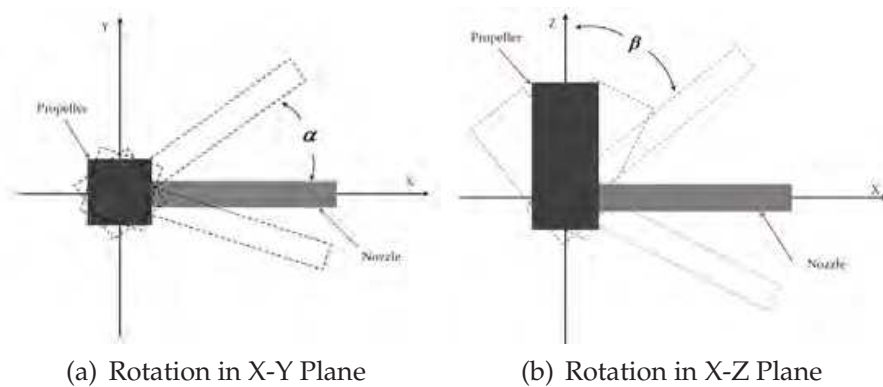


Fig. 10. Orientation of Propellers

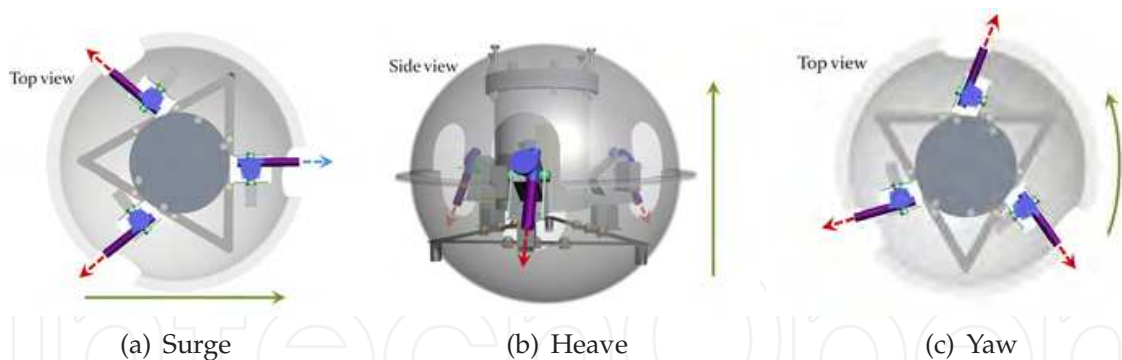


Fig. 11. Propulsion Forces for Surge, Heave and Yaw

The first case is surge. In this case, two of the water-jet propellers will work together, and the other one could be used for brake. So, from Fig.11(a), two water-jet propellers in the left will be used for propulsion, and if we want to stop the vehicle from moving, the third propeller can act as a braking propeller. From Equation 4, the resultant force for surge can be expressed in vehicle-fixed coordinate as:

$$\begin{cases} {}^p F_{xb} = \Phi_{p1}^{bT} \sum_{i=1}^3 ({}^p F_{ip} + \mathbf{e}_1 C_i) \neq 0 \\ {}^p F_{yb} = 0 \\ {}^p F_{zb} = 0 \end{cases} \quad (5)$$

where,  $\mathbf{e}_1 = (1, 0, 0)^T$ .

Then, for the heave case, all the three water-jet propellers will work and the side servo motor will rotate to an angle that  $\beta > \pi/2$ . Therefore, in this case, the resultant force for heave can be expressed in vehicle-fixed coordinate as:

$$\begin{cases} {}^pF_{xb} = 0 \\ {}^pF_{yb} = 0 \\ {}^pF_{zb} = \Phi_{p3}^{bT} \sum_{i=1}^3 ({}^pF_{ip} + \mathbf{e}_3 C_i) \neq 0 \end{cases} \quad (6)$$

where,  $\mathbf{e}_3 = (0, 0, 1)^T$ .

The third case is yaw which is rotating on z-axis. By denoting in propeller-fixed coordinates,  $\alpha$  should have the same orientation, clockwise or counterclockwise, that means,  $\alpha_i > 0$  or  $\alpha_i < 0$ . So in yaw, rotation moment will take effect. We can write the equation for yaw in vehicle-fixed coordinate as:

$$\begin{cases} {}^pF_{xb} = \Phi_{p1}^{bT} \sum_{i=1}^3 ({}^pF_{ip} + \mathbf{e}_1 C_i) \neq 0 \\ {}^pF_{yb} = \Phi_{p2}^{bT} \sum_{i=1}^3 ({}^pF_{ip} + \mathbf{e}_2 C_i) \neq 0 \\ {}^pF_{zb} = 0 \\ {}^pM_{xb} + {}^pM_{yb} + {}^pM_{zb} \neq 0 \end{cases} \quad (7)$$

where,  $\mathbf{e}_2 = (0, 1, 0)^T$ ,  $\mathbf{e}_3 = (0, 0, 1)^T$ .

### 3.2 Modeling of single water-jet propeller

In the author's previous research (Guo et al., 2009), the modeling for orientation of water-jet propeller is presented. Therefore, in this part, we will only discuss about the hydrodynamics modeling of the water-jet thruster. The method we refer to is presented in (Kim & Chung, 2006). For the purpose of dynamic modeling of water-jet propeller, we give the flow model of the water-jet thruster, which is shown in Fig.12. The shaft is perpendicular to the nozzle, and there are two blades.

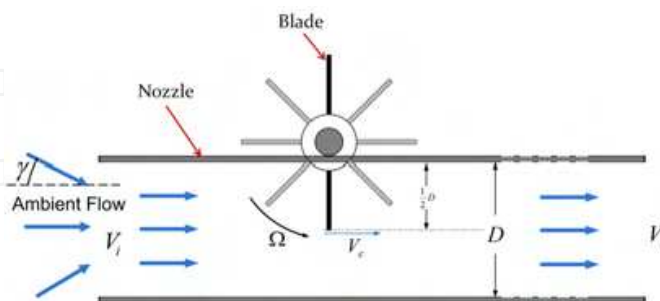


Fig. 12. Flow Model of the Water-jet Thruster (top view)

where,

$\Omega$  is angular velocity of the thruster

$V_i$  is velocity of incoming flow

$V_c$  is central flow velocity in the nozzle

$D$  is diameter of the nozzle

$V_o$  is velocity of outlet flow

$\gamma$  is incoming angle of ambient flow

Because the diameter of the nozzle is small, the velocity difference in the nozzle can be ignored, so we consider the axis flow velocity  $V_a$  as a linear combine of incoming flow velocity and the central flow velocity,

$$\begin{aligned} V_a &= k_1 V_i + k_2 V_c \\ V_c &= \frac{1}{2} D \Omega \\ V_i &= V_f \cos \gamma \end{aligned} \quad (8)$$

By assuming that the flow is incompressible, therefore, from equation of continuity, we know that the volume of incoming flow must equal to the outlet flow, then we get:

$$\rho_a V_a A_a = \rho_o V_o A_o \quad (9)$$

where,  $\rho_a = \rho_o$  is density of flow,  $A_a = A_o$  is cross-section of the nozzle.

Therefore, we can also get:

$$V_a = V_o \quad (10)$$

Meanwhile, we know that, the propulsive force of the water-jet thruster is:

$$F_t = \rho A V_a^2 \quad (11)$$

By substituting Equation 8 in Equation 11, we can get:

$$F_t = \frac{\pi}{4} \rho D^2 (k_1^2 V_i^2 + 2k_1 k_2 V_i D \Omega + k_2^2 D^2 \Omega^2) \quad (12)$$

By rewriting Equation 12, we get:

$$\frac{F_t}{\rho D^4 \Omega^2} = \frac{\pi}{4} (k_1^2 (\frac{V_i}{D \Omega})^2 + 2k_1 k_2 \frac{V_i}{D \Omega} + k_2^2) \quad (13)$$

Then, we can let the non-dimensional parameter be:

$$K_T(J_0) = \frac{\pi}{4} (k_1^2 (\frac{V_i}{D \Omega})^2 + 2k_1 k_2 \frac{V_i}{D \Omega} + k_2^2) \quad (14)$$

where

$$J_0 = \frac{V_i}{D \Omega} = \frac{V_f \cos \gamma}{D \Omega} \quad (15)$$

$J_0$  is the advance ratio.

Now, the modeling becomes measuring of three parameters, flow velocity, incoming angle and angular velocity of thruster. For this purpose, we designed an experiment to measure these parameters and find out their relationship.

Flow velocities	Depth	Incoming angles	Control voltages
0.1m/s	80cm	0 – $\pi$	3V – 7V (DC)
0.2m/s			

Table 1. Experiment Condition

### 3.3 Experiments for the dynamics modeling

In this part, we try to identify the dynamics model of the water-jet propeller by experiment. What we are interested in is the relation of flow incoming angles, flow velocities and propulsive forces. Experiment condition is listed in Table 1.

#### 3.3.1 Experiment design

Fig.13 gives the experiment principle. We use one NEC 2301 stain gage as the force sensor and use NEC AC AMPLIFIER AS 1302 to amplify the output signal from strain gage, which are shown in Fig.14.

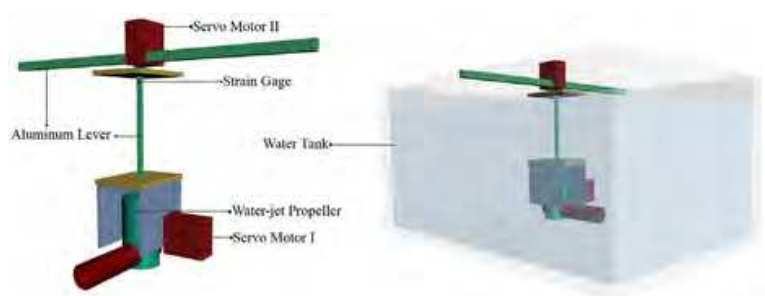


Fig. 13. Experiment Design for Identification



Fig. 14. Strain Gage and Amplifier

Firstly, we give a brief illustration for the strain gage measurement. Let  $F_d$  be deformation force, and  $\epsilon$  be the deformation of aluminium lever used in the experiment. Therefore, from the theory of mechanics of materials, we can get the relation of  $F_d$  and  $\epsilon$  as:

$$F_d = \frac{ZE}{X}\epsilon \quad (16)$$

where,  $Z$  is second moment of area,  $E$  is the Young's modulus,  $X$  is the distance from acting point of force to stain gage.

#### 3.3.2 Experiments and analysis

In the experiment, there are four variables we need to consider, the equivalent cross-section of propeller, flow velocity, incoming angle and control voltage. What we are interested in is the variation of propulsive force in different incoming angles and different control voltage.

### 3.3.2.1 Equivalent cross-section variation of propellers

As a vectored water-jet-based propulsion system, it should be noted that both the propulsive force and its direction can be changed. Therefore, when the propeller changes its direction, actually, the incoming angle of flow is also changing, and the equivalent cross-section of the propeller is changing. From Equation 11 we know the propulsive force will change if cross-section  $A$  changes. Fig.15 gives a demonstration of this case. When the propeller rotate from position I to II, the equivalent cross-section will change from cross-section I to cross-section II. So we try to find an equation to describe this variation.

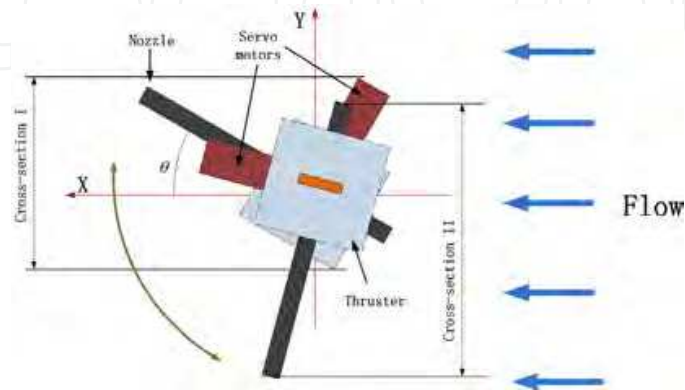


Fig. 15. Variation of Equivalent Cross-section of Propellers

Considering that the measured force from strain gage is actually a resultant force of propulsive force and fluid force. And we also know that the fluid force acted on the propeller depends on the equivalent cross-section.

So the first experiment is measurement of the equivalent cross-section variation. The propeller is submerged in the flow which has a speed of  $0.2m/s$ , propeller is powered off. And we only change its orientation in  $X - Y$  plane. Because of experiment limits, we can not change the flow direction, so in the experiment, the incoming angle equals to the orientation angle of the propeller. Fig.15 gives a demonstration of the equivalent cross-section. We give some special angles,  $0, \pi/6, \pi/3, 2\pi/3, 5\pi/6, \pi$ , for this experiment. Fig.16 gives the experiment data of equivalent cross-section. You may notice that, we did not adopt the orientation angle of  $\pi/2$ . Because, when the propeller rotate to  $\pi/2$ , which means that the measure surface of the strain gage is parallel to the flow direction, the strain gage can not measure the flow force.

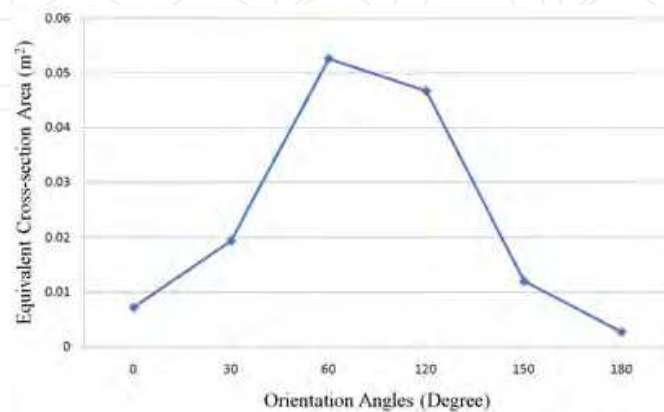


Fig. 16. Variation of Equivalent Cross-section

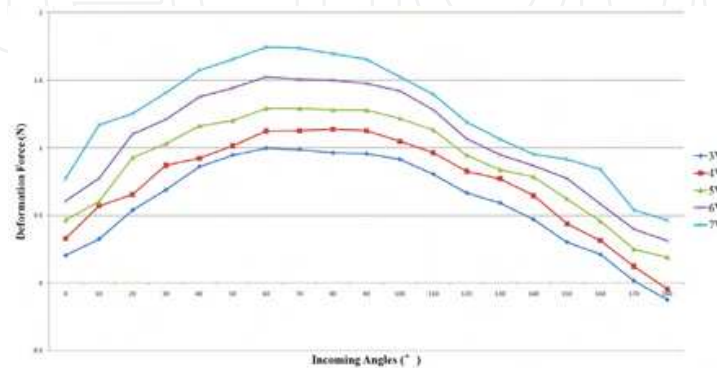
From Fig.16 we can see, the data curve is similar with a sinusoid, so we use a sine function to fit this experiment data:

$$A_e(\phi) = \lambda_1 \sin(\lambda_2 \phi + \lambda_3) \quad (17)$$

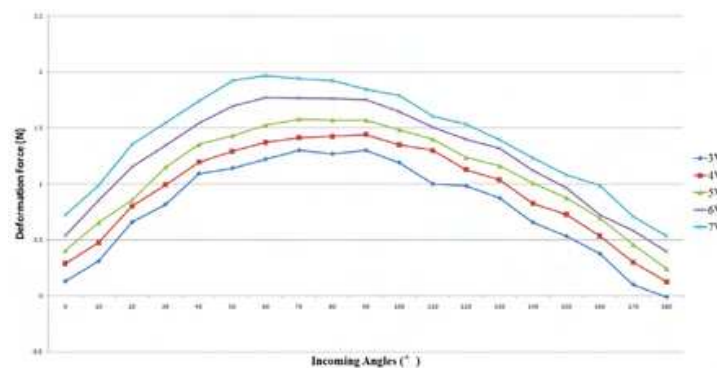
where  $\phi$  is incoming angle,  $\lambda_1, \lambda_2, \lambda_3$  are coefficients.

### 3.3.2.2 Incoming angle and deformation force

In this case, the flow velocity is seen as constant. Two groups of experiment are carried out at flow velocity of  $0.1m/s$  and  $0.2m/s$ . The control voltage to thruster is from  $3V$  to  $7V$  every  $1V$ . From the data shown in Fig.17, we can see that the deformation force does not simply increase



(a)  $V_f = 0.1m/s$



(b)  $V_f = 0.2m/s$

Fig. 17. Deformation Forces with Different Incoming Angles

with the increasing of incoming angle, the maximum deformation of the lever happens at about 60 degree of the incoming angles. They are not a linear relation. Then, how about the real propulsive force?

### 3.3.2.3 Incoming angle and propulsive force

As we mentioned, what we measured by stain gage is actually a resultant force of propulsive force and fluid force. Therefore, the real propulsive force  $F_t$  should be calculated using deformation force  $F_d$  and the equivalent cross-section  $A_e$ .

$$F_d = F_t - F_f \cos \gamma \quad (18)$$

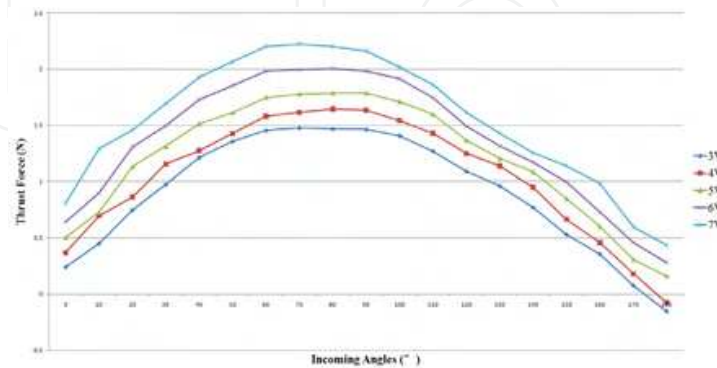
If we consider about the fluid force of the flow, we can refer to Equation 11 and 17, then write the fluid force as:

$$F_f = \rho V_c^2 A_e(\phi) \quad (19)$$

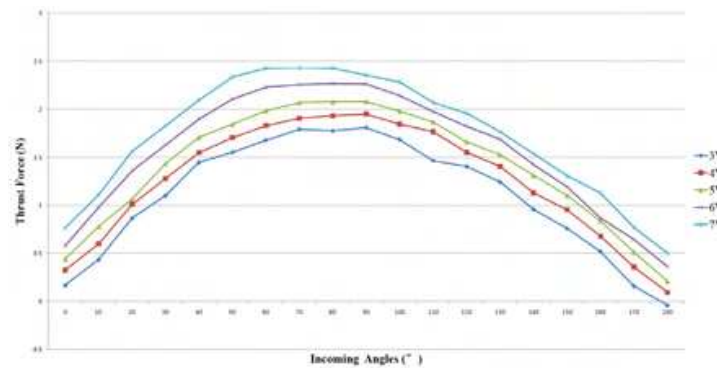
We substitute Equation 19 into 18 we get:

$$F_t = F_d + \rho V_c^2 A_e(\phi) \cos \gamma \quad (20)$$

So now, we can calculate the real propulsive force by using equivalent cross-section, deformation force and incoming angles. The results is shown in Fig.18. Fig.18(a) and Fig.18(b) are results at the flow velocity of  $V_f = 0.1m/s$  and  $V_f = 0.2m/s$ , respectively.



(a)  $V_f = 0.1m/s$



(b)  $V_f = 0.2m/s$

Fig. 18. Propulsive forces with Different Incoming Angles

#### 3.3.2.4 Control voltage and propulsive force

From the results of 3.3.2.3, we can obtain the relation of control voltage and propulsive force. First, we give the experiment data, in Fig.19. From the diagram, we can see that the relation of control voltage and propulsive force can be described using linear equation.

### 4. Underwater experiments for basic motions

Because of the symmetrical shape of the hull, it is obvious that motion characteristics of surge, sway and heave should be similar. However, from another point of view, surge and sway are motions in  $X - Y$  plane while heave is a motion that its motion surface perpendicular to  $X - Y$  plane. Therefore, we carry out experiments for horizontal motion surface and vertical motion surface respectively. Besides, for the experimental prototype vehicle, we only consider one rotational DOF in  $Z$  axis, so the third experiment is yaw motion.

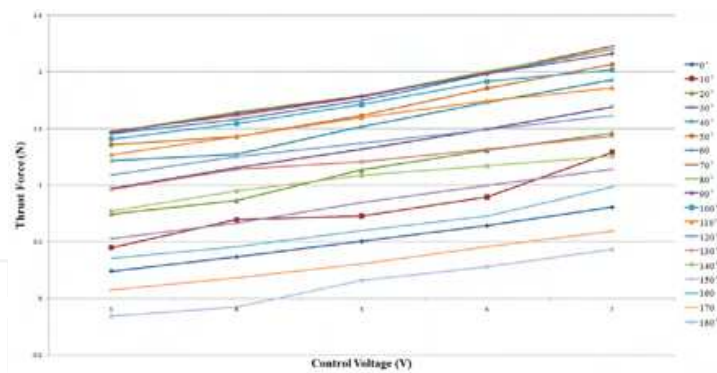
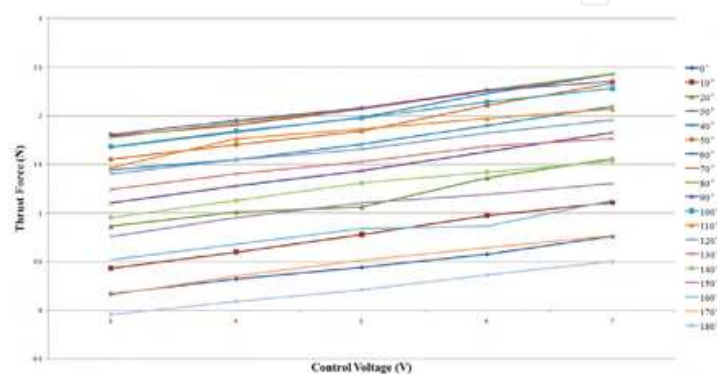
(a)  $V_f = 0.1m/s$ (b)  $V_f = 0.2m/s$ 

Fig. 19. Propulsive forces with Different Control Voltages

#### 4.1 Experiment of horizontal motion

This experiment combines surge and sway together to verify the motion characteristics of the vehicle in horizontal plane. We carried out three experiments:

##### Case 1:

- step 1. Surge (Move forward in X axis);
- step 2. Right steering (Turn right about  $90^\circ$ );
- step 3. Sway (Move forward along Y axis.)

##### Case 2:

- step 1. Surge (Move forward in X axis);
- step 2. Left steering (Turn left about  $90^\circ$ );
- step 3. Sway (Move forward along Y axis.)

##### Case 3:

- step 1. Surge (Propeller I and II work together, propeller III powered off);
- step 2. Brake (Propeller I and II powered off, Propeller III works to produce brake force).

In case 1, timing of step 1 is about 10s, and step 2 takes about 12s. And timing of case 2 is relatively the same with case 1, because of the same hydrodynamics characteristics of turning right and left. In case 3, it takes 15s reaching a stable speed, and the brake effect happens in about 3s which is effective for low speed underwater vehicles. From Fig.20, we can see,

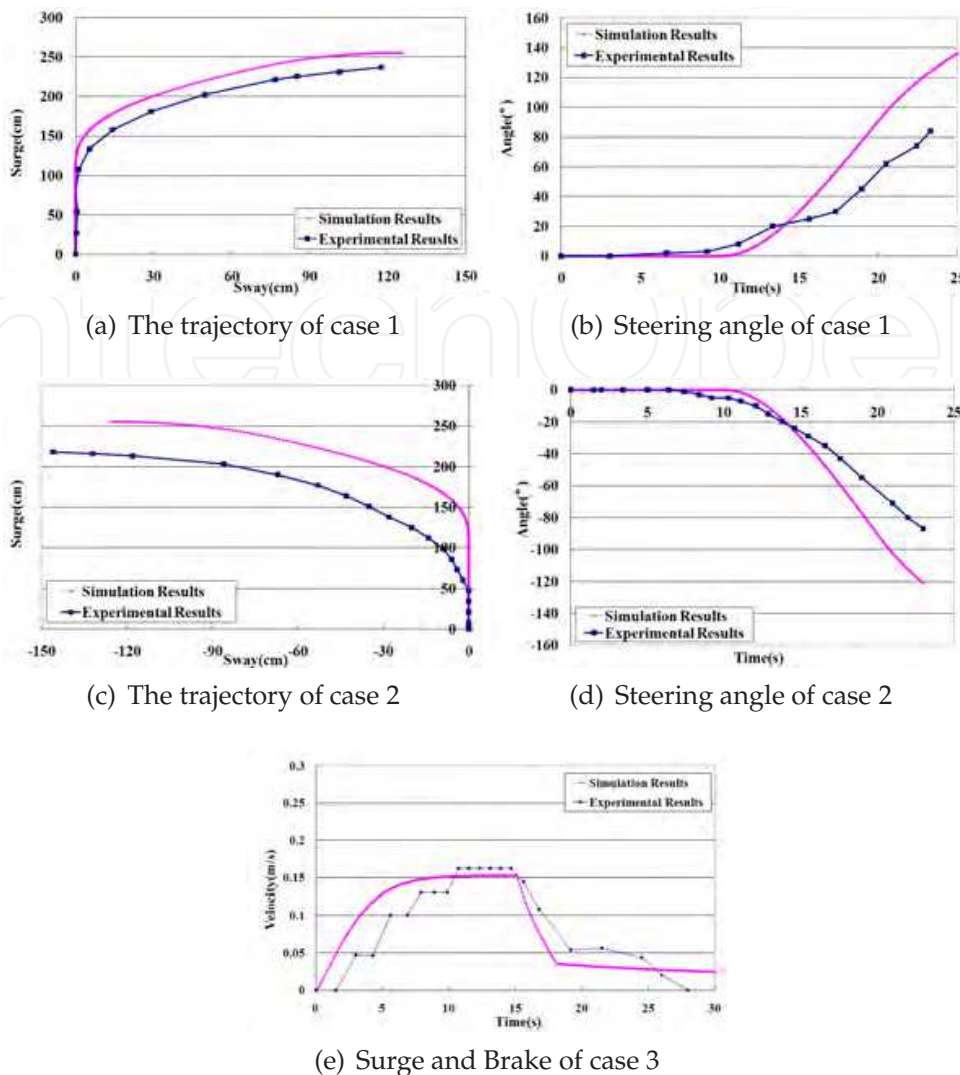


Fig. 20. Experimental Results of Horizontal Motion

the experimental results fit well with simulation results in surge stage, but when the vehicle rotating, errors become large. The reason of this is because the simulation experiment only considered linear damping force and quadratic damping force, but in reality, there are other hydrodynamic forces act on the vehicle.

#### 4.2 Experiment of vertical motion

Even though we design the working depth of the vehicle to  $10m$ , because the depth of experimental pool is only  $1.2m$ , we can only make the experiments in shallow water. So we set the vertical motion time in a relatively small range. We also carried out two experiments:

##### Case 1:

- step 1. Set the top point of the spherical hull as the start point;
- step 2. Move downward in Z axis for about  $7s$  ;
- step 3. Float up to the surface.

##### Case 2:

- step 1. Set the top point of the spherical hull as the start point;

step 2. Move downward in Z axis for about 7s ;

step 3. Stop the vehicle.

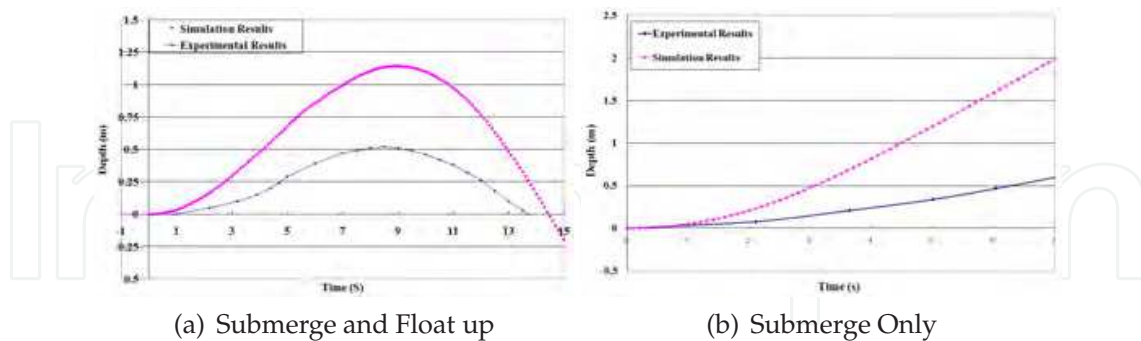


Fig. 21. Experimental Results of Vertical Motion

From Fig.21(a) and Fig.21(b), we can see, the experimental results does not fit well with simulation results very well, errors exceed 100%. When we analyze the reasons, we find that, the simulation experiment does not consider the variation of water pressure. The control voltage to the thrusters is 7V as a constant. That means, the propulsive force will not change. But with the increasing of depth, water pressure increases. As a result, the effective propulsive force are weakened by water pressure.

#### 4.3 Experiment of yaw

We let the vehicle rotate about  $90^\circ$  then stop. From Fig.22(a) and Fig.22(b), the maximum error between simulation results and experimental results happens at about 2.8s where is nearly the maximum angular velocity. The reason of this result is that, we simplified the model of our vehicle, especially the hydrodynamic damping forces. Only linear damping force and quadratic damping force are taken into account in our case. But in the real experiment, there are many other velocity related hydrodynamic damping forces, therefore, when the angular velocity increasing, the damping effect of ignored forces become obvious.

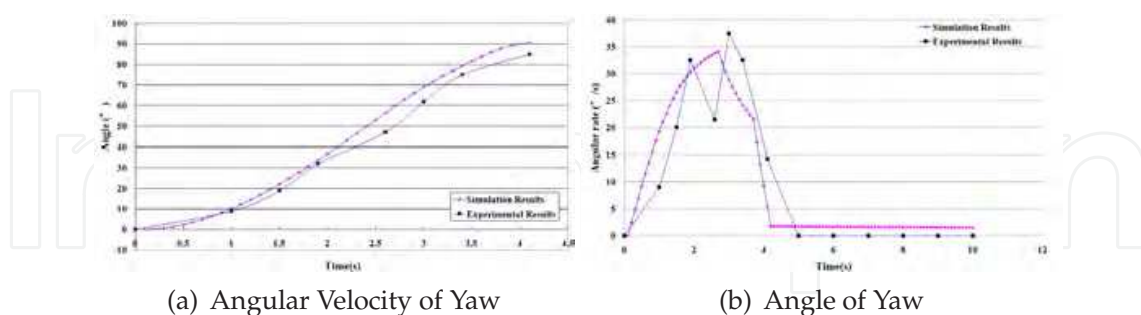


Fig. 22. Experimental Results of Yaw

## 5. Conclusions

In this paper, we proposed a spherical underwater vehicle which uses three water-jet propellers as its propulsion system. We introduced the design details of mechanical and electrical system.

Based on the design of the vehicle, we introduced the principles of the water-jet propulsion system including the force distribution of three water-jet propellers, the working principles of different motions. And then we discussed about the modeling of one single propeller by identification experiments. For the modeling, the flow velocity and equivalent cross-section of the propeller are taken into account for dynamics model.

One experimental prototype of this spherical underwater vehicle is developed for the purpose of evaluation. Underwater experiments are carried out to evaluate the motion characteristics of this spherical underwater vehicle. Experimental results are given for each experiment, and the analysis are also given.

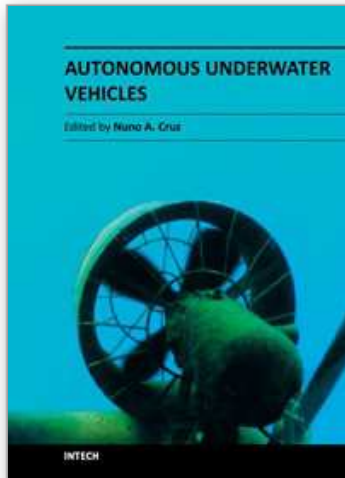
From the underwater experiments of the prototype vehicle, the availability of the design is proved, and the water-jet propulsion system can work well for different motions. But there are also some problems needed to be resolved. Firstly, the propulsive force of the water-jet propellers needed to be increased; secondly, the variation of water pressure on the propulsive force should be considered when building the dynamics model of propellers; thirdly, the gravity distribution should be re-regulated to improve stability; finally, from experiments, it is necessary to improve the accuracy of the dynamics model of the vehicle for precise control.

## 6. References

- Allen, B., Stokey, R., Austin, T., Forrester, N., Goldsborough, R., Purcell, M. & von Alt, C. (2002). REMUS: a small, low cost AUV; system description, field trials and performance results, *OCEANS'97. MTS/IEEE Conference Proceedings*, Vol. 2, IEEE, pp. 994–1000.
- Antonelli, G. & Chiaverini, S. (2002). Adaptive tracking control of underwater vehicle-manipulator systems, *Proceedings of the 1998 IEEE International Conference on Control Applications*, 1998, Vol. 2, IEEE, pp. 1089–1093.
- Antonelli, G., Chiaverini, S., Sarkar, N. & West, M. (2002). Adaptive control of an autonomous underwater vehicle: experimental results on ODIN, *IEEE Transactions on Control Systems Technology* 9(5): 756–765.
- Beal, B. (2004). *Clustering of Hall effect thrusters for high-power electric propulsion applications*, PhD thesis, The University of Michigan.
- Blanke, M., Lindegaard, K. & Fossen, T. (2000). Dynamic model for thrust generation of marine propellers, *Proceedings of the IFAC Conference on Maneuvering and Control of Marine Craft (MCMC 2000)*, Citeseer.
- Cavallo, E., Micheli, R. & Filaretov, V. (2004). Conceptual design of an AUV Equipped with a three degrees of freedom vectored thruster, *Journal of Intelligent & Robotic Systems* 39(4): 365–391.
- Duchemin, O., Lorand, A., Notarianni, M., Valentian, D. & Chesta, E. (2007). Multi-Channel Hall-Effect Thrusters: Mission Applications and Architecture Trade-Offs, *30th International Electric Propulsion Conference*, Florence, Italy.
- Fossen, T. I. (1995). *Guidance and Control of Ocean Vehicles*, John Wiley & Sons Ltd., USA.
- Guo, S., Lin, X. & Hata, S. (2009). A conceptual design of vectored water-jet propulsion system, *International Conference on Mechatronics and Automation, 2009. ICMA 2009*, IEEE, pp. 1190–1195.
- Kim, J. & Chung, W. (2006). Accurate and practical thruster modeling for underwater vehicles, *Ocean Engineering* 33(5-6): 566–586.
- Kowal, H. (2002). Advances in thrust vectoring and the application of flow-control technology, *Canadian aeronautics and space journal* 48(2): 145–151.

- Lazic, D. & Ristanovic, M. (2007). Electrohydraulic thrust vector control of twin rocket engines with position feedback via angular transducers, *Control Engineering Practice* 15(5): 583–594.
- Le Page, Y. & Holappa, K. (2002a). Hydrodynamics of an autonomous underwater vehicle equipped with a vectored thruster, *OCEANS 2000 MTS/IEEE Conference and Exhibition*, Vol. 3, IEEE, pp. 2135–2140.
- Le Page, Y. & Holappa, K. (2002b). Simulation and control of an autonomous underwater vehicle equipped with a vectored thruster, *OCEANS 2000 MTS/IEEE Conference and Exhibition*, Vol. 3, IEEE, pp. 2129–2134.
- Madhan, R., Desa, E., Prabhudesai, S., Sebastião, L., Pascoal, A., Desa, E., Mascarenhas, A., Maurya, P., Navelkar, G., Afzulpurkar, S. et al. (2006). Mechanical design and development aspects of a small AUV–Maya, *7th IFAC Conference MCMC2006*.
- Newman, J. (1977). *Marine hydrodynamics*, The MIT press.
- Sangekar, M., Chitre, M. & Koay, T. (2009). Hardware architecture for a modular autonomous underwater vehicle STARFISH, *OCEANS 2008*, IEEE, pp. 1–8.

IntechOpen



## **Autonomous Underwater Vehicles**

Edited by Mr. Nuno Cruz

ISBN 978-953-307-432-0

Hard cover, 258 pages

**Publisher** InTech

**Published online** 17, October, 2011

**Published in print edition** October, 2011

Autonomous Underwater Vehicles (AUVs) are remarkable machines that revolutionized the process of gathering ocean data. Their major breakthroughs resulted from successful developments of complementary technologies to overcome the challenges associated with autonomous operation in harsh environments. Most of these advances aimed at reaching new application scenarios and decreasing the cost of ocean data collection, by reducing ship time and automating the process of data gathering with accurate geo location. With the present capabilities, some novel paradigms are already being employed to further exploit the on board intelligence, by making decisions on line based on real time interpretation of sensor data. This book collects a set of self contained chapters covering different aspects of AUV technology and applications in more detail than is commonly found in journal and conference papers. They are divided into three main sections, addressing innovative vehicle design, navigation and control techniques, and mission preparation and analysis. The progress conveyed in these chapters is inspiring, providing glimpses into what might be the future for vehicle technology and applications.

### **How to reference**

In order to correctly reference this scholarly work, feel free to copy and paste the following:

Shuxiang Guo and Xichuan Lin (2011). Development of a Vectored Water-Jet-Based Spherical Underwater Vehicle, *Autonomous Underwater Vehicles*, Mr. Nuno Cruz (Ed.), ISBN: 978-953-307-432-0, InTech, Available from: <http://www.intechopen.com/books/autonomous-underwater-vehicles/development-of-a-vectored-water-jet-based-spherical-underwater-vehicle>

**INTECH**  
open science | open minds

#### **InTech Europe**

University Campus STeP Ri  
Slavka Krautzeka 83/A  
51000 Rijeka, Croatia  
Phone: +385 (51) 770 447  
Fax: +385 (51) 686 166  
[www.intechopen.com](http://www.intechopen.com)

#### **InTech China**

Unit 405, Office Block, Hotel Equatorial Shanghai  
No.65, Yan An Road (West), Shanghai, 200040, China  
中国上海市延安西路65号上海国际贵都大饭店办公楼405单元  
Phone: +86-21-62489820  
Fax: +86-21-62489821

© 2011 The Author(s). Licensee IntechOpen. This is an open access article distributed under the terms of the [Creative Commons Attribution 3.0 License](#), which permits unrestricted use, distribution, and reproduction in any medium, provided the original work is properly cited.

IntechOpen

IntechOpen